Lagrangian Motion of Particles and Tracers on Isopycnals

MEI-MAN LEE

James Rennell Division, Southampton Oceanography Centre, Southampton, United Kingdom

(Manuscript received 27 November 2000, in final form 20 November 2001)

ABSTRACT

This study looks at the behavior of fluid particles/parcels that move along isopycnic surfaces. The aim is to show that the diffusive process of mixing by eddies causes such particles to move toward regions of greater isopycnic layer thickness or, equivalently, weaker stratification.

This is illustrated using a wind-driven eddy-resolving isopycnic layer model in a zonal channel configuration. Particles and tracers are integrated to demonstrate that their centers of mass move *up* the layer thickness gradient. In particular, a field of uniformly distributed particles is seen to move toward regions of large layer thickness, so the distribution of particles becomes asymmetric. The asymmetry is most obvious when the gradient of layer thickness is large in comparison to the volume of the layer. In the ocean, in the absence of other influences such as advection and varying diffusivity, one might expect isopycnic floats released in the upper thermocline to show a similar asymmetric behavior.

1. Introduction

Tracers and floats are commonly used for identifying water mass pathways and mixing characteristics in the ocean. For example, hydrographic surveys and isopycnic floats reveal that the Gulf Stream seems to act as a barrier, separating slope water from Saragasso Sea water in the upper thermocline, but at the same time acts as a mixer in the deep thermocline (Bower et al. 1985; Bower and Rossby 1989).

Theoretical and numerical studies on the motion of fluid particles/parcels, thought of as small fluid volumes rather than as individual fluid molecules, are motivated in order to have a better understanding of float movement and tracer distribution. It is known that the behavior of fluid particles is influenced by energetic eddies. Rhines (1977) showed that fluid particles move preferentially towards regions of large diffusivity in the absence of advection. Similarly, it has been shown in atmospheric models that the center of mass of a set of dispersing air particles tends to move toward regions where eddy activity is relatively strong (Dunkerton et al. 1981).

Given that properties in the ocean (temperature, salinity, and chemical tracers) are primarily transported and mixed along isopycnals, this paper will study the motion of fluid particles (and tracers) along isopycnals. In particular, it will be shown that the diffusive process of mixing by eddies causes fluid particles to move toward regions of greater isopycnic layer thickness.

This result may be summarized using the following thought experiment. In an isopycnic layer, the fluids are initially divided into columns with equal widths (Fig. 1a). As the result of eddy mixing, fluid columns are redistributed (Fig. 1b). Since the volume of each fluid column is conserved, initially thin columns are stretched when they move to thicker regions and, conversely, initially thick columns are flattened when they move to thinner regions. As particles move with the fluid columns, the mixing of fluid columns results in the initially uniform distribution of particles becoming nonuniform (the black dots in Fig. 1). Thus, particles appear to have a tendency to move toward regions where the isopycnic layer thickness is greater.

In this paper, such behavior will be explained from theory and demonstrated using numerical models. Section 2 derives the motion of the center of mass of tracers and of isopycnic fluid particles, showing that the motion is controlled by total advection (mean and eddy), eddy diffusivity, and layer thickness. In particular, when there is no total advection and diffusivity is constant, this motion is controlled by the layer thickness gradient. This is demonstrated by integrating tracers and particles in an isopycnic model. Section 3 describes the wind-driven eddy-resolving model configurated in a zonal channel. Section 4 shows the motion of particles and tracers. Section 5 discusses the implication of the study for tracers and floats in the ocean.

Corresponding author address: Dr. Mei-Man Lee, James Rennell Division, Southampton Oceanography Centre, Southampton SO14 3ZH, United Kingdom.
E-mail: mmlee@soc.soton.ac.uk

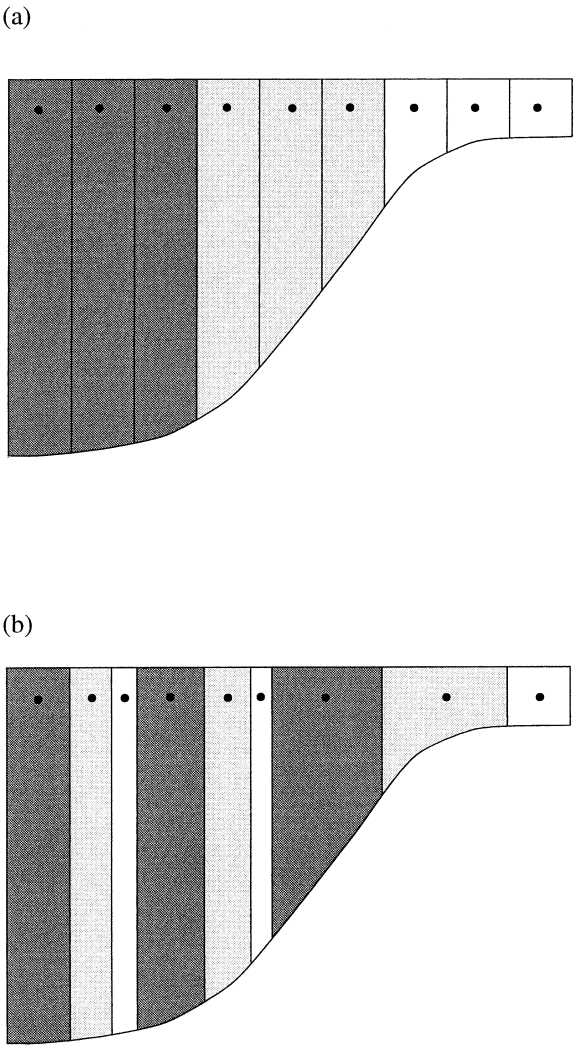

FIG. 1. Schematic of an isopycnic layer in an eddying flow. (a) An initial distribution of fluid columns. The black dots are particles that move with the fluid columns. (b) The fluid columns have been redistributed by the eddy mixing. Conservation of the volume of each column results in a nonuniform distribution of particles.

2. Motion of the center of mass

a. Tracers

For stably stratified fluids, the conservation of tracer substance can be expressed in isopycnic coordinates as

$$\frac{\partial}{\partial t}(Ch) + \nabla \cdot (\mathbf{u}Ch) = 0, \tag{1}$$

where C is the tracer concentration defined as the tracer substance per unit mass, $h = -\partial z/\partial\rho$ (z is the height of isopycnal and ρ is the density), $\mathbf{u}$ is the horizontal velocity, and ∇ is the horizontal gradient operator at constant ρ (assuming no diapycnic flow). By definition, the thickness of the layer between isopycnal surfaces ρ and $\rho + \delta\rho$ is $h\delta\rho$. However, for convenience, h will be referred to as layer thickness (per unit density).

Equation (1) is the conservation equation for any tracer. For example, it can be the conservation of salt substance where C is the salt concentration (i.e., salinity). It also applies to some dynamical tracers such as potential vorticity (PV). It has been suggested that potential vorticity can be thought of as the concentration of PV substance (Haynes and McIntyre 1990). Thus, if C is the potential vorticity concentration, then Eq. (1) is just the absolute vorticity equation.

Applying averaging operators to (1) gives

$$\frac{\partial}{\partial t}(\overline{Ch}) + \nabla \cdot (\hat{\mathbf{u}}\overline{Ch}) = \nabla \cdot (\overline{h}\mathbf{K} \cdot \nabla\hat{C}). \tag{2}$$

The averaging operator (overbar) can be either spatial or temporal. The caret is the corresponding layer-thickness-weighted averaging operator, $\hat{\varphi} = \overline{\varphi h}/\overline{h}$. Here, $\mathbf{K}$ is the eddy diffusion tensor given by $\widehat{\mathbf{u}^*C^*} = -\mathbf{K} \cdot \nabla\hat{C}$, where $\varphi^* = \varphi - \hat{\varphi}$ is the deviation from the weighted averaging. The derivation of (2) is straightforward and a similar equation can be found in Dukowicz and Greatbatch (1999).

Consider a domain where there is no normal flow through the lateral boundary and $\mathbf{K} = 0$ at the boundary. Multiplying (2) by $\mathbf{x} = (x, y)$ and integrating over the domain, the lateral motion of the center of (tracer) mass in an isopycnal layer is

$$\mathbf{u}_c \equiv \frac{\partial[\mathbf{x}]}{\partial t} = [\hat{\mathbf{u}}] + \left[\frac{1}{\overline{h}}\nabla \circ (\overline{h}\mathbf{K})\right], \tag{3}$$

where

$$[\cdot] = \int (\cdot)\overline{Ch}\, d\mathbf{x} \Big/ \int \overline{Ch}\, d\mathbf{x}$$

is an average using the mean tracer substance and the notation $\nabla\circ$ is the divergence of row vectors of the matrix.

The first term on the rhs of (3) is the thickness-weighted mean advection, which includes the mean velocity, $\overline{\mathbf{u}}$, and the eddy-induced "bolus" velocity, $\mathbf{u}_B = \overline{\mathbf{u}'h'}/\overline{h}$, where $\varphi' = \varphi - \overline{\varphi}$. The second term is the thickness-weighted gradient of the eddy diffusion tensor. It can be shown that the motion $\mathbf{u}_c$ is closely related to the generalized Lagrangian mean velocity (Andrews and McIntyre 1978). More details are in the appendix.

Now, consider the situation where $\hat{\mathbf{u}} = 0$ and $\mathbf{K} = \kappa\mathbf{I}$ (where κ is the diffusivity and $\mathbf{I}$ is the identity matrix), then (3) reduces to $\mathbf{u}_c = [(1/\overline{h})\nabla(\overline{h}\,\kappa)]$. Given this, there are three special cases.

1) *h and κ are constant.* In this case, $\mathbf{u}_c = 0$ and so the center of mass does not move.
2) *h is constant.* In this case, $\mathbf{u}_c = [\nabla\kappa]$. The center of mass moves preferentially toward the regions of large diffusivity. This reproduces the result of Rhines (1977).
3) *κ is constant.* In this case, $\mathbf{u}_c = [(\kappa/\overline{h})\nabla\overline{h}]$ and so

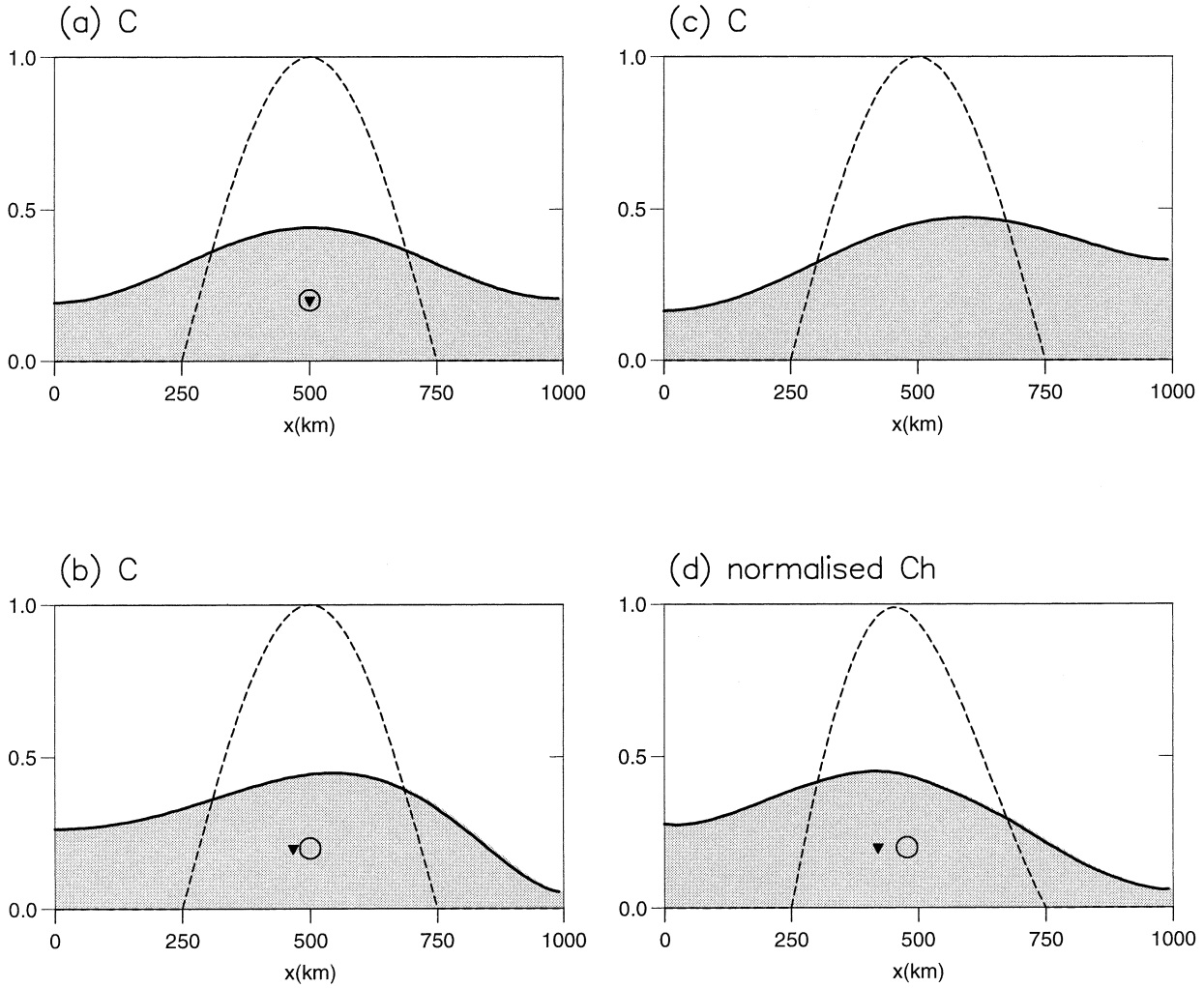

FIG. 2. The solutions of (4) for three cases. The broken lines are the initial values. The shaded regions in (a), (b), (c) are the final tracer concentrations. The shaded region in (d) is normalized tracer substance, *Ch*, for (c). The open circles and triangles are the initial and final positions of the center of mass. Three cases: (a) Diffusivity and layer thickness are constant, showing a symmetric spreading of concentration and so there is no motion of the center of mass. (b) Layer thickness is constant but diffusivity increases to the left, showing the center of mass moves to the left where diffusivity is larger. (c) Diffusivity is constant but layer thickness increases to the left, showing a higher concentration to the right. The normalized tracer substance in (d) shows that the center of mass moves to the left where the layer is thicker.

the center of mass moves toward large layer thickness.

These three cases can be demonstrated using a simple example. Consider the one-dimensional diffusion equation,

$$\frac{\partial C}{\partial t} = \frac{1}{h}\frac{\partial}{\partial x}\left(h\kappa\frac{\partial C}{\partial x}\right), \tag{4}$$

in a domain of size 1000 km and no flux through the boundaries. The grid spacing is 10 km and the time step is 1200 s. The concentration C is initialized with a sinusoidal profile over the middle 500 km and the numerical solutions after 30 000 time steps are shown in Fig. 2.

In the first case, layer thickness h and diffusivity κ are constant ($\kappa = 1000$ m^2 s^{-1}). The concentration spreads symmetrically and the center of mass does not move (Fig. 2a). In the second case, diffusivity κ increases linearly from 100 to 2000 m^2 s^{-1} toward the left. The concentration increases to the left, so the center of mass moves toward the left where the diffusivity is larger (Fig. 2b). In the third case, diffusivity is kept constant but the layer thickness h increases linearly from 100 to 900 m toward the left. The concentration, C, shown in Fig. 2c, is higher to the right. However, this does not imply that the center of mass is to the right. Figure 2d shows the normalized tracer substance, *Ch*. As expected from (3) above, the center of mass moves to the left where h is larger.

It can be seen from (4) that the asymmetric tendency of center of mass is due to the layer-thickness-weighted

diffusive flux, $h\kappa\partial C/\partial x$, that is, the total diffusive flux in an isopycnic layer. Larger layer thickness implies more diffusive flux, leading to more tracer substance. This phenomenon is physical and would also be observed in (x, y, z) coordinates providing the diffusion is along isopycnals. However, the isopycnic framework is clearer and more intuitive in the sense that, when tracer concentrations are diffused toward the homogeneous state, the center of mass of the tracer is the center of mass of the layer, which is toward the thicker part of the layer.

So eddies diffuse the center of mass of tracer toward the region of large layer thickness. It is worth comparing this to the eddy-induced bolus velocity, $\overline{\mathbf{u}}_B$, which is often associated with slumping isopycnals due to baroclinic instability. Thus, eddy-induced advection tends to be down the layer thickness gradient, that is, toward regions where the layer is *thinner*. The downgradient eddy advection has been used for parameterization in ocean models (Gent and McWilliams 1990; Gent et al. 1995). It has been shown that eddy-induced advection can enhance or inhibit the spreading of tracers from a source region (Lee et al. 1997).

It is interesting to note that in terms of the motion of the center of mass two eddy processes oppose each other—eddy advection moves the center of mass toward the thinner part of the layer, whereas eddy diffusion moves it toward the thicker part. It can be shown that, in the limit of small-amplitude perturbations, they have the same order of magnitude (see the appendix). Therefore, the eddy advection and eddy diffusion in (3) are equally important in controlling the motion of the center of mass of tracer.

b. Isopycnic particles

Here, a fluid *particle* is to be understood as an infinitesimal volume element containing many molecules, though still regarded as a point. In an isopycnic layer, fluid moves as a column since velocity is vertically uniform. Thus, an isopycnic fluid particle at $\mathbf{x}$ following $\mathbf{u}(\mathbf{x})$ represents the horizontal motion of the volume element that has an infinitesimal horizontal area and whose height is the local layer thickness. When the particle moves to a new position, the area of the fluid column changes in inverse proportion to the layer thickness so that the volume is conserved.

Now, imagine a fixed amount of dye substance injected into the fluid. Fluid particles represent volume elements containing the dye substance. When the fluid particles move, they simply carry the dye substance to the new location. Therefore, the motion of the center of mass for the fluid particles is the same as that for the substance, that is, Eq. (3).

As it is important to distinguish tracer concentration from tracer substance, it should be emphasized again that concentration is by definition the amount of substance (i.e., number of fluid particles) per unit mass. Hence, the same number of fluid particles corresponds to a lower concentration in a thicker region than in a thinner region.

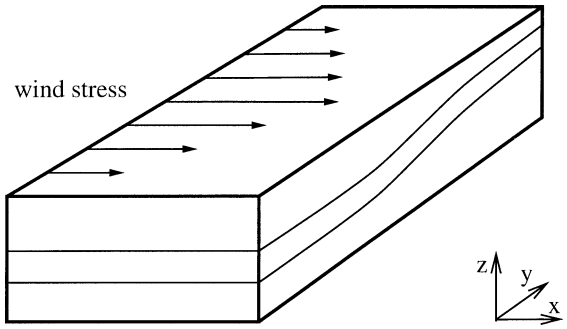

FIG. 3. Schematic of the model.

In the following, an idealized model is used to demonstrate the motion of the fluid particles and to compare this motion to that of the tracers.

3. Model

A zonally periodic isopycnic layer model (MICOM v2.6) is configured with dimensions of 600 km east–west, 1000 km north–south, and 2000 m deep. The spatial resolution is 10 km. There are three isopycnic layers with potential densities $\sigma = 26.0$, 26.5, and 27.0 kg m^{-3}. The initial layer thickness in the top layer is 100 m at the northern boundary and 900 m at the southern boundary. The middle layer thickness is 500 m. The model is forced by a zonal wind $\tau_0 \sin(\pi y/L)$ where $\tau_0 = 0.1$ N m^{-2} and L is the north–south extent (Fig. 3). The Coriolis parameter is $f = f_\circ + \beta y$ where $f_\circ = 0.83 \times 10^{-4}$ s^{-1} and $\beta = 2 \times 10^{-11}$ m^{-1} s^{-1}. The bottom drag is given by $c_d(|\mathbf{u}_a| + c)\mathbf{u}_a$, where $c_d = 0.003$ is the drag coefficient, $c = 0.1$ m s^{-1} and $\mathbf{u}_a$ is the velocity of bottom layer.

The model is first run for 2 years to reach a statistically steady state. Then, tracers and particles are released to be integrated for further 10 years. The mean quantities are diagnosed by taking zonal and temporal averaging over 10 years. The thickness-weighted mean zonal velocity, $\hat{u}$, reaches 30 cm s^{-1} in the top layer (Fig. 4a). The wind-driven Ekman flow is southward ($\overline{v} \sim -0.3$ cm s^{-1}) in the top layer with a returning frictionally driven northward flow in the bottom layer (Fig. 4b). With Ekman pumping to the south and Ekman suction to the north, isopycnals rise to the north. The baroclinic eddies act to flatten the isopycnals, giving a northward eddy-induced bolus advection ($v_B \sim +0.3$ cm s^{-1}) in the top layer and a reversed flow in the bottom layer (Fig. 4c). There is no thickness-weighted mean flow ($\hat{v} = 0$) since the Ekman flow is completely cancelled by the eddy flow. In the real ocean the thickness-weighted mean flow is not necessarily zero. However, this configuration allows a clear illustration of the idea of this study.

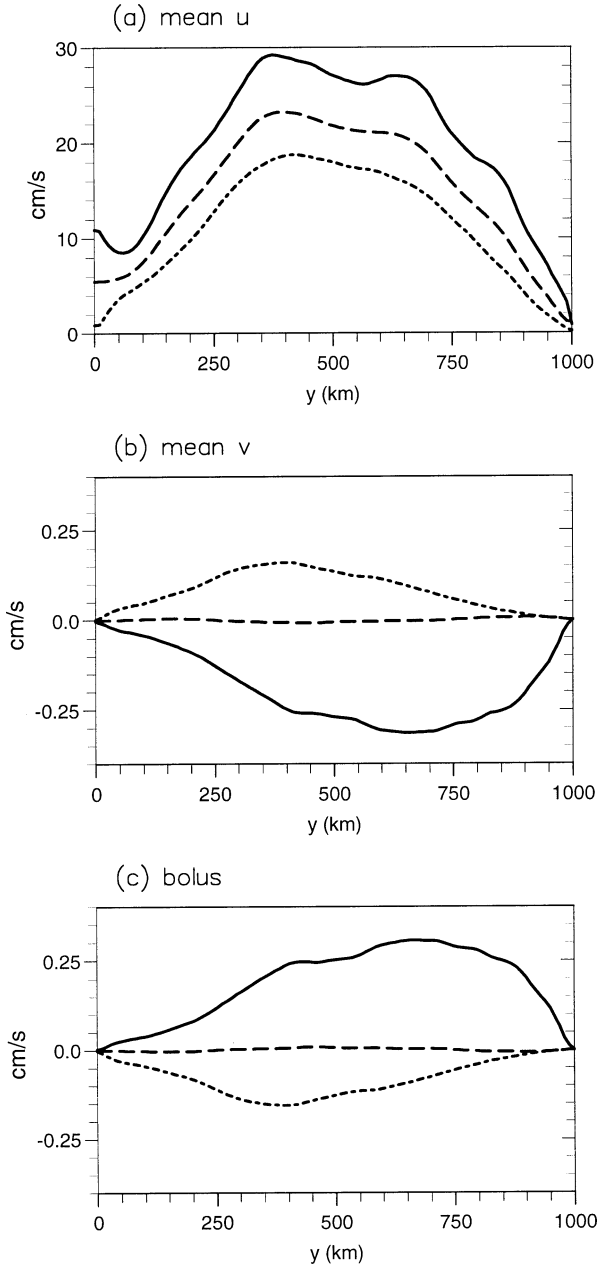

FIG. 4. The zonally and temporally averaged velocity (cm s^{-1}): (a) thickness-weighted mean zonal velocity $\hat{u}$, (b) mean meridional velocity $\overline{v}$, and (c) meridional bolus velocity v_B. The solid, broken, and dotted line indicates the top, middle, and bottom layer.

4. Tracer and particles

There are 6000 particles seeded uniformly with one particle at the center of each model grid. The particles are integrated forward using a fourth-order Runge–Kutta method and bilinear interpolation for the velocities at the particle positions. Tracer concentration is initialized as $c \times 1/h$, where c is a normalization constant, so tracer has the maximum value 1. This ensures that the tracer and particles are initialized in a consistent manner since one particle represents one unit of tracer substance, which is equivalent to concentration $1/h$.

a. Displacement of center of mass

The tracer concentration at day 5 (Fig. 5) shows the eddy activities in all three layers. After 10 years, tracers in all layers are homogenized by eddies (not shown).

After 5 days, the particle distributions are distorted locally (Fig. 6, top panels). After 10 years, the particle distribution is different in each layer (Fig. 6, bottom panels). In the top layer, the distribution is asymmetric with most of the particles accumulated in the southern half of the domain. In the middle layer the distribution is fairly uniform and in the bottom layer the distribution is slightly asymmetric with perhaps relatively more particles on the northern half of the domain.

The particle distribution can be quantified by summing up the number of particles in each zonal band. The number is 60 at day 0 and the number at year 10 is shown in Fig. 7 (solid lines). In the top layer, the number of particles increases to the south and decreases to the north, indicating a southward net motion of particles. In the middle layer, the number of particles is close to 60, indicating almost no net motion. In the bottom layer, the net motion is northward. This ilustrates that particles tends to move toward regions where the layer is thicker.

This can be compared with the tracer. The tracer substance at each zonal band is just the mean layer thickness scaled by a constant since concentration is uniform. Thus, particles are expected to correlate with layer thickness since they also represent tracer substance. Figure 7 shows the mean layer thickness (broken lines) superimposed on the number of particles (solid lines). The two are well-correlated, confirming that particle distribution is consistent with the uniform tracer concentration.

The displacements of the center of mass are now examined by following the meridional position of the center of mass over the 10-year period (Fig. 8a). For the tracer, the center of mass moves southward in the top layer (solid line) and northward in the middle and bottom layers (broken line and dotted line).

The center of mass for the particles shows a similar displacement (Fig. 8a, markers). However, the particles seem to give a larger displacement compared to the tracer. This is probably due to sampling problems. In the present experiment, tracer will never be zero whereas particles can disappear from a thinner layer thickness region completely. When this happens, particles at a thinner region become underrepresented so that the center of mass appears to move farther. Despite this problem, the two calculations agree well to give a consistent motion of center of mass toward the region where the layer is thicker.

The displacement is largest in the top layer and smallest in the middle layer. The different amounts of dis-

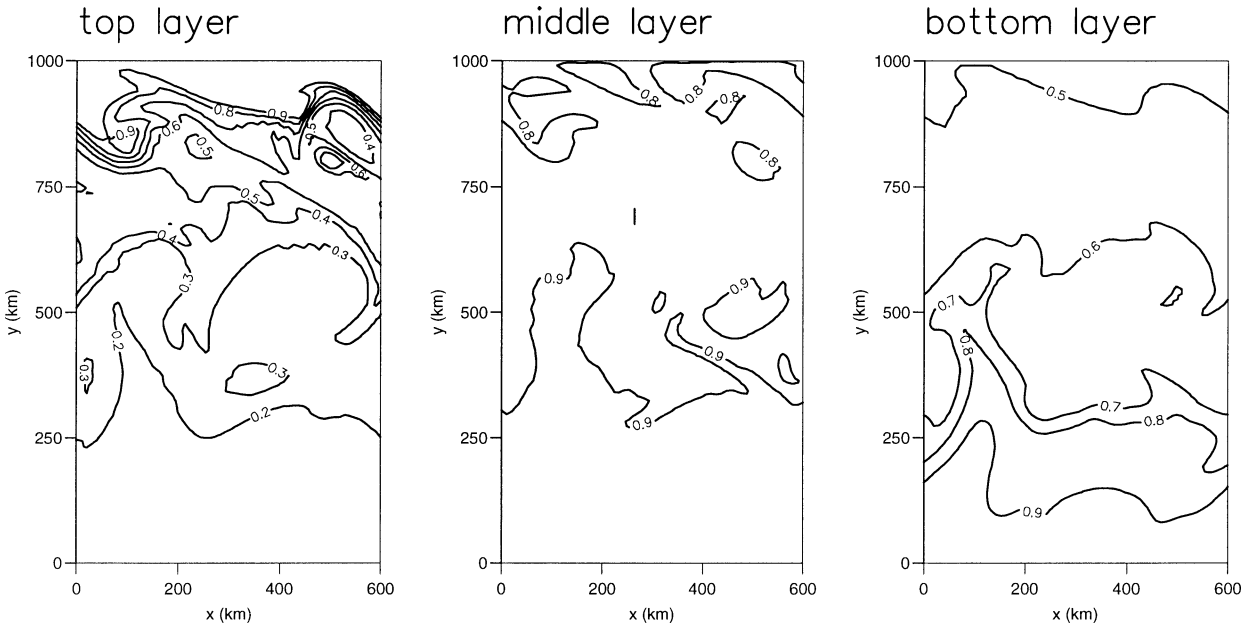

FIG. 5. The tracer fields at day 5. The contour intervals are 0.1.

placement can be explained as follows. At year 10, the center of mass for tracer is just the center of mass of the layer since tracer concentration is uniform. Therefore, the amount of displacement depends on how far the center of mass of the layer is away from the center of the channel. This distance can be roughly estimated by the ratio, $(h_n - h_s)/(h_n + h_s)$, where h_n and h_s is the layer thickness at the north and south boundaries. A larger ratio implies a greater displacement. This ratio is 0.8, 0.15, and -0.31 for the top, middle, and bottom layer, which is consistent with the largest displacement in the top layer and smallest displacement in the middle layer.

b. How is the net motion controlled?

Here, the terms in (3) are diagnosed to examine what controls the motion of the center of mass. The diagnostics are for the top layer only since it has the largest displacement of the center of mass.

For zonal averaging, the meridional motion of the center of mass is

$$v_c \equiv \frac{d[y]}{dy} = [\hat{v}] + \left[\frac{1}{\overline{h}}\frac{\partial}{\partial y}(\overline{h}\kappa)\right], \qquad (5)$$

where κ is the eddy diffusivity satisfying $\widehat{v^*C^*} = -\kappa\partial\hat{C}/\partial y$. As seen in Fig. 8a, the motion of center of mass is time-dependent. For this reason, the temporal averagings are carried out over 60-day time spans.

For the first 2 years, v_c is about -0.1 cm s^{-1} (Fig. 8b, heavy solid line). During this period, the advection term, $[\hat{v}]$ (light broken line), is very small as expected. Therefore the motion of the center of mass is mainly due to the thickness-weighted gradient of diffusivity.

Note that the bolus velocity contribution $[v_B] \sim +0.2$ cm s^{-1} (not shown) is comparable to v_c. This confirms that bolus velocity and the thickness-weighted gradient of diffusivity have the same order of magnitude, but with opposite signs.

After 5 years, $v_c \sim [\hat{v}]$. This is because when tracer approaches a uniform value, the second term on the right hand side of (5) vanishes; that is,

$$\left[\frac{1}{\overline{h}}\frac{\partial(\overline{h}\kappa)}{\partial y}\right] = \int \frac{\partial(\overline{h}\kappa)}{\partial y}\,dy \Big/ \int \overline{h}\,dy = 0,$$

assuming κ is zero at boundary.

The second term on the rhs of (5) can be separated into two terms,

$$\left[\frac{1}{\overline{h}}\frac{\partial}{\partial y}(\overline{h}\kappa)\right] = \left[\frac{\kappa}{\overline{h}}\frac{\partial\overline{h}}{\partial y}\right] + \left[\frac{\partial\kappa}{\partial y}\right]. \qquad (6)$$

The first term is related to the gradient of layer thickness and the second term is the gradient of diffusivity. These two terms are also shown in Fig. 8b. They are calculated for the first 3 years, after which the diffusivity κ becomes undefined. Since most of the displacement of the center of mass occurs at the first 3 years (Fig. 8a shows a displacement of 80 km in 3 years comparing to 140 km in 10 years), the diagnostics from this period should be sufficient.

The thickness gradient term (heavy dotted line) is about -0.15 cm s^{-1}, which is similar to v_c. The diffusivity gradient term (light broken-dotted line) is only about $+0.05$ cm s^{-1}. Therefore the motion of the center of mass cannot be due to the diffusivity gradient. To be certain of this, the diffusivity κ is shown in Fig. 8c, confirming no obvious correlation between diffusivity

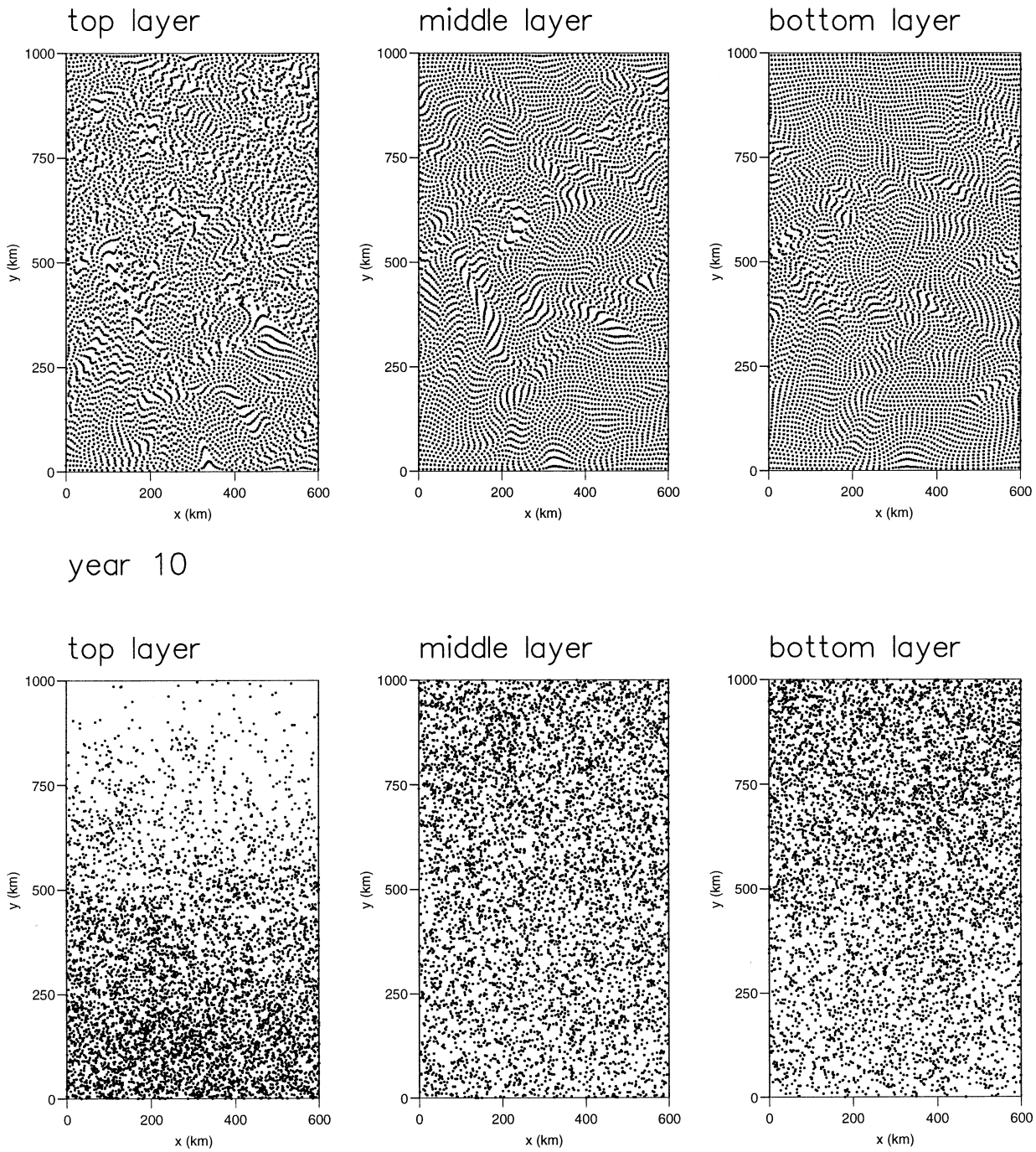

FIG. 6. The particle distribution at day 5 (top panels) and year 10 (bottom panels) in three layers. After 10 years, the particles in the top layer move toward south whereas particles in the bottom layer move toward north.

and layer thickness. Thus, the movement of particles toward the large layer thickness is mainly due to the gradient of layer thickness.

c. Particle exchanges

The motion of the center of mass is independent of the rate of particle exchange since there can be many particles moving across but no net displacement of the center of mass. To clarify this, particles in the experiment are divided into two groups. The southern (northern) group contains those particles originating from the southern (northern) half. After 10 years, the number of particles from each group moving to the other side is counted.

In the top layer, there are 349 particles from the south-

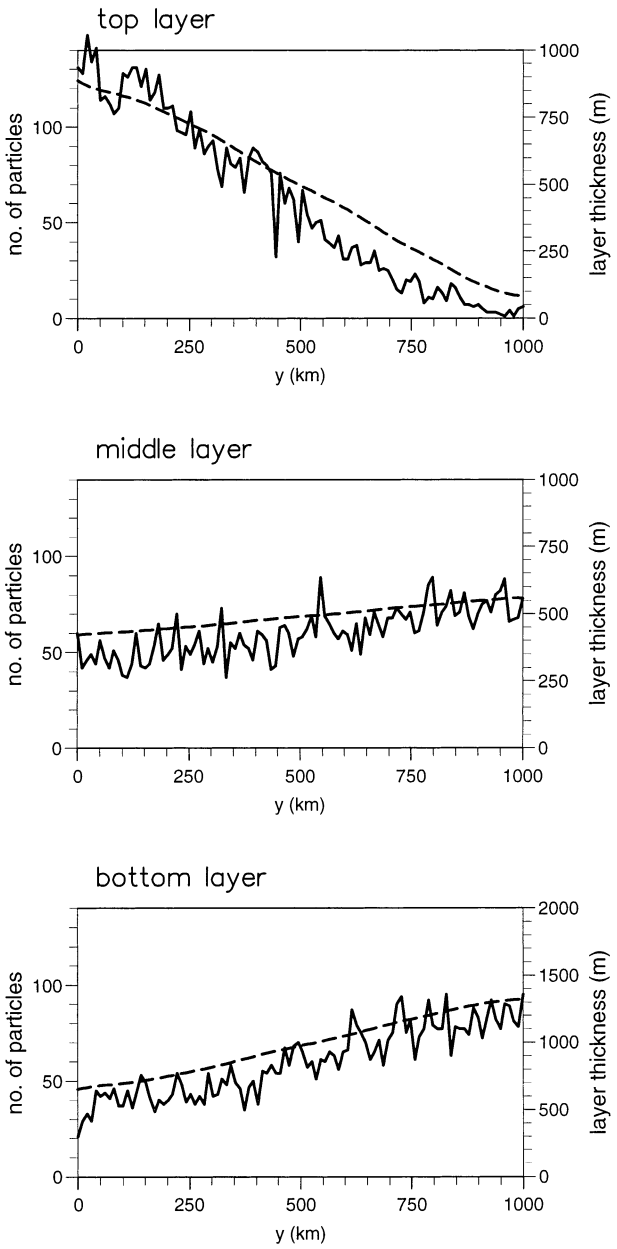

FIG. 7. The solid lines are the number of particles in each zonal band at year 10. The broken lines are the mean layer thicknesses (m).

ern group moving to the north whereas 2285 particles from the northern group are moving to the south. The particle exchanges are largely in one direction—from north to south. In the bottom layer, there are 1100 particles moving from north to south and 1832 particles moving from south to north. The exchanges are in both directions, implying fairly uniform mixing. This is almost consistent with Bower et al. (1985) where they showed from hydrographic sections in the Gulf Stream that water masses mixing is stronger in the deep thermocline than in the upper themocline. However, the zonal jet in the experiment is not completely a ''barrier''

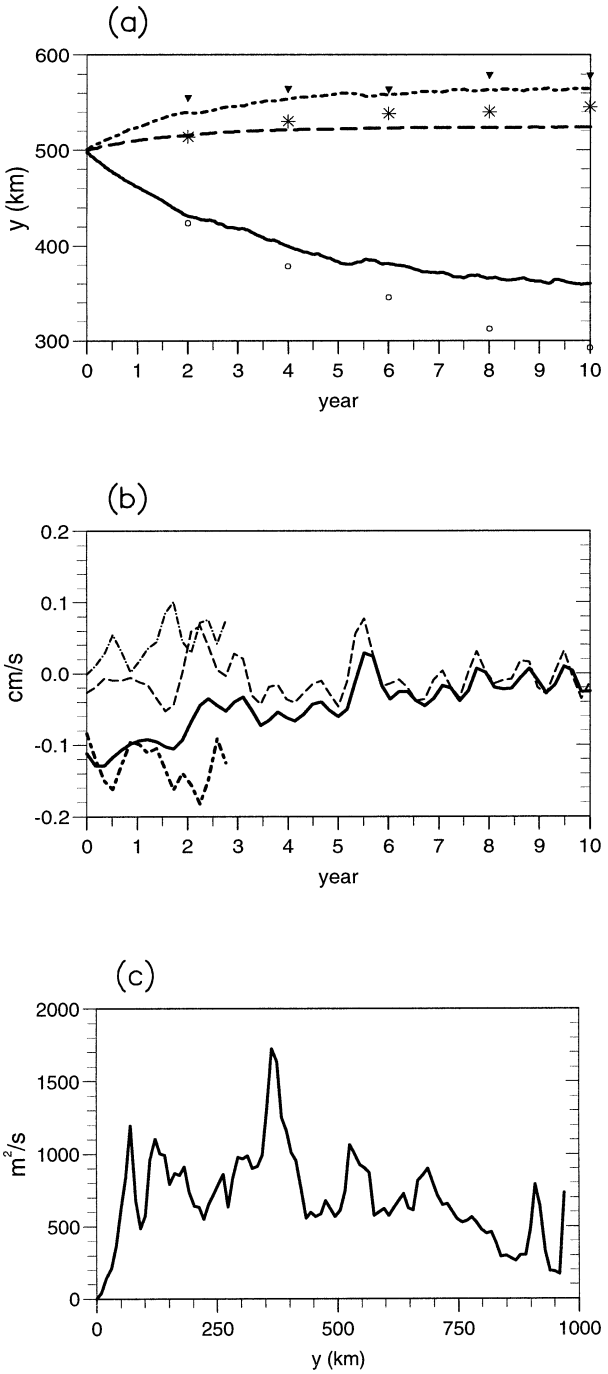

FIG. 8. (a) The time series of the meridional position of the center of mass. Lines are from the tracers. The solid, broken, and dotted line indicates the top, middle, and bottom layer. Markers are from the particles. The open circles, stars and triangles indicate the respective layer. (b) The diagnostics of the terms in (5) and (6) for the top layer. The terms are calculated using zonal and temporal averaging over 60-day time spans. The heavy solid line is $v_c \equiv d[y]/dt$, the light broken line is $[\hat{v}]$, the heavy dotted line is $[\kappa/\overline{h}\,\partial\overline{h}/\partial y]$, and the light broken-dotted line is $[\partial\kappa/\partial y]$. (c) Diffusivity κ ($m^2\ s^{-1}$) in the top layer plotted as a function of y. It was diagnosed using a zonal and temporal averaging for the first 2 years.

in the sense that more than 70% of the particles in the top layer cross the jet from north to south. This seems to suggest that the zonal jet in the upper layer is like a ''one-way barrier.''

5. Summary and discussion

In the ocean, water mass properties and tracers are primarily transported and mixed along isopycnals. In terms of following tracers and particles, it is useful to think in an isopycnic framework. This study shows that the motion of the center of mass of tracers and particles is controlled by the thickness-weighted mean advection, $\hat{\mathbf{u}}$, and the thickness-weighted gradient of eddy diffusivity, $h^{-1}\nabla(\kappa h)$.

Under the conditions of no thickness-weighted mean advection and constant eddy diffusivity, fluid particles will be diffused toward the region of greater layer thickness or, equivalently, weaker stratification. This is illustrated by numerical experiments where an initially uniform distribution of particles becomes asymmetric with more particles to the thicker part of the layer. This may be compared to other diffusive effects of eddies. It is known that eddies diffuse particles toward the region of large diffusivity (Rhines 1977). This study demonstrated that eddy diffusion can also cause the particles to move toward the region of large layer thickness.

Eddies also have an advective role. Eddy-induced advection (bolus velocity) is essentially *down* the gradient of mean layer thickness. This is in contrast to eddy diffusion, which leads to the motion of particles *up* the gradient of mean layer thickness. Therefore, the two eddy processes oppose each other in moving the center of mass. However, the operation of eddy diffusion relies on nonvanishing tracer gradients. So eddy diffusion stops operating when tracers are uniform. On the other hand, eddy advection is always present as long as there exists a layer thickness gradient.

The asymmetric behavior of fluid particles is a physical phenomenon that does not depend on the coordinates. A similar behavior can also be observed in (x, y, z) coordinates providing the conservation of tracer substance along isopycnals is strictly obeyed. For numerical models, it requires eddy diffusion to be along isopycnals.

This study focused on the effect of layer thickness and so excluded the effects of advection and diffusivity. In the ocean, thickness-weighted mean advection and spatially varying diffusivity are likely to be dominant, so the asymmetric distribution of particles may not be observable. However, the asymmetric behavior of isopycnic fluid particles has not been addressed before and may be useful for interpreting isopycnic floats in the regions where the conditions are appropriate.

Consider isopycnic floats released in some isopycnic layer of thickness similar to the height of the floats, typically 1 m. Thus, isopycnic floats are analogous to the numerical particles in the model since both move with the vertically averaged velocity in the layer. This paper showed that the tendency of the fluid particles is controlled by the ratio $\Delta h/h$ (note that this ratio remains the same after dividing an isopycnic layer into sublayers). Therefore, in the upper thermocline where $\Delta h/h$ is large (e.g., top model layer), float distribution would be more asymmetric with a tendency to move to the thicker side of the layer. In the deep thermocline where $\Delta h/h$ is small (e.g., bottom model layer), floats from either sides of the layer can get across and therefore the distribution would be more uniform.

When comparing tracers in the ocean with isopycnic floats, it should be borne in mind that floats are to be compared with tracer substance and not with tracer concentration. Again, this distinction is particularly important in the regions where the ratio $\Delta h/h$ is large.

Acknowledgments. This study is supported by the EU MAST-3 program TRACMASS CT970142. I thank Alastair King, Peter Killworth, and George Nurser for helpful discussions, and Rainer Bleck and Linda Smith for providing the numerical code.

APPENDIX

Generalized Lagrangian Mean Velocity in Isopycnic Coordinates

The motion of the center of mass is a Lagrangian mean motion. It can be related to the generalized Lagrangian mean (GLM) velocity (Andrews and McIntyre 1978), which describes the motion of the center of mass for a string of particles that initially lay undisturbed along the direction of averaging.

The GLM velocity can be derived explicitly in the limit of small-amplitude perturbations. The most familiar version is in z coordinates, but an isopycnic version for zonal averaging is also partly provided by Andrews et al. (1987) for atmospheric jets and by Boss and Thompson (1999) for normal-mode waves in a two-layer ocean model.

Here, the GLM velocity is derived in isopycnic coordinates. Consider the mean state to be $\hat{\mathbf{u}}$, $\hat{C}$, and $\overline{h}$, and the perturbations, $\mathbf{u}^*$, C^*, and h', to be of order α (a measure of perturbation amplitude). Following Andrews and McIntyre (1978), let $\boldsymbol{\xi} = (\xi, \eta)$ be the Lagrangian particle displacement that satisfies,

$$\overline{\boldsymbol{\xi}} = 0,$$

$$\frac{\partial \boldsymbol{\xi}}{\partial t} + (\hat{\mathbf{u}} \cdot \nabla)\boldsymbol{\xi} = \mathbf{u}^* + (\boldsymbol{\xi} \cdot \nabla)\hat{\mathbf{u}} + O(\alpha^2). \quad \text{(A1)}$$

Perturbed continuity and tracer equations are

$$\frac{\partial h'}{\partial t} + \nabla \cdot (\hat{\mathbf{u}}h') + \nabla \cdot (\mathbf{u}^*\overline{h}) = O(\alpha^2), \quad \text{(A2)}$$

$$\frac{\partial C^*}{\partial t} + \hat{\mathbf{u}} \cdot \nabla C^* + \mathbf{u}^* \cdot \nabla \hat{C} = O(\alpha^2). \quad \text{(A3)}$$

Substitute $\mathbf{u}^*$ in (A2), (A3) using (A1) to deduce

$$h' + \nabla \cdot (\boldsymbol{\xi}\overline{h}) = O(\alpha^2), \quad \text{(A4)}$$

$$C^* + \boldsymbol{\xi} \cdot \nabla \hat{C} = O(\alpha^2). \quad \text{(A5)}$$

In this way, the perturbations are related to the displacement. This is the isopycnic version of Hayes (1970) and Andrews and McIntyre (1978).

From (A4) and (A5),

$$\overline{\mathbf{u}'h'} = -\mathbf{K} \cdot \nabla \overline{h} - \mathbf{u}'\overline{h}\nabla \cdot \boldsymbol{\xi} + O(\alpha^2), \quad \text{(A6)}$$

$$\widehat{\mathbf{u}^*C^*} = -\mathbf{K} \cdot \nabla \hat{C} + O(\alpha^3), \quad \text{(A7)}$$

where

$$\mathbf{K} = \begin{pmatrix} \widehat{\xi u^*} & \widehat{\eta u^*} \\ \widehat{\xi v^*} & \widehat{\eta v^*} \end{pmatrix}.$$

Note that (A7) implies that eddy tracer flux, $\widehat{\mathbf{u}^*C^*}$, can be parameterized as down the gradient of mean tracer $\hat{C}$ whereas (A6) implies that the eddy layer thickness flux, $\overline{\mathbf{u}'h'}$, cannot be parameterized as down the mean layer thickness gradient because of the extra term in (A6). This feature has been reported by others using different approaches (Treguier et al. 1996; Killworth 1997; Dukowicz and Greatbatch 1999),

The generalized Lagrangian mean velocity is defined as $\overline{\mathbf{u}}^{\mathrm{L}} = \overline{\mathbf{u}(\mathbf{x} + \boldsymbol{\xi})}$. Apply Taylor's expansion to the right-hand side to obtain

$$\overline{\mathbf{u}}^{\mathrm{L}} = \overline{\mathbf{u}} + \overline{(\boldsymbol{\xi} \cdot \nabla)\mathbf{u}^*} + \frac{1}{2}\overline{\boldsymbol{\xi} \cdot (\boldsymbol{\xi} \cdot \nabla)}\nabla\hat{\mathbf{u}} + O(\alpha^3). \quad \text{(A8)}$$

The second term on the right-hand side of (A8) can be rearranged by multiplying by $\overline{h}$ and dividing by $\overline{h}$ again. For example, the zonal component becomes

$$\overline{(\boldsymbol{\xi} \cdot \nabla)u^*} = \frac{\overline{u^*h'}}{\overline{h}} + \frac{1}{\overline{h}}\nabla \cdot (\overline{h}\,\overline{\boldsymbol{\xi}u^*}), \quad \text{(A9)}$$

where (A4) is used to obtain the first term on the right-hand side of (A9).

Substitute (A9) to (A8) and use $\mathbf{u}^* = \mathbf{u}' + O(\alpha^2)$ to obtain

$$\overline{u}^{\mathrm{L}} = \overline{u} + \frac{\overline{u'h'}}{\overline{h}} + \frac{1}{\overline{h}}\nabla \cdot (\overline{h}\,\overline{\boldsymbol{\xi}u^*}) + \frac{1}{2}\overline{\boldsymbol{\xi} \cdot (\boldsymbol{\xi} \cdot \nabla)}\nabla\hat{u} + O(\alpha^3).$$

A similar expression can be obtained for the meridional component. Therefore,

$$\overline{\mathbf{u}}^{\mathrm{L}} = \overline{\mathbf{u}} + \frac{\overline{\mathbf{u}'h'}}{\overline{h}} + \frac{1}{\overline{h}}\nabla \circ (\overline{h}\mathbf{K}) + \frac{1}{2}\overline{\boldsymbol{\xi} \cdot (\boldsymbol{\xi} \cdot \nabla)}\nabla\hat{\mathbf{u}} + O(\alpha^3). \quad \text{(A10)}$$

First, this confirms the claim in section 2 that the eddy diffusion and eddy-induced advection have the same order of magnitude. Second, this shows that the GLM velocity and the motion of the center of mass derived in (3) are similar. However, the third term on the right hand side of (A10), which is related to the nonlinearity of the mean velocity, does not appear in (3). Unfortunately, it is not clear how to interprete this difference.

Finally, the Stokes drift $\overline{\mathbf{u}}^{\mathrm{S}}$ can be defined as

$$\overline{\mathbf{u}}^{\mathrm{L}} = \overline{\mathbf{u}} + \overline{\mathbf{u}}^{\mathrm{S}}.$$

Thus, with respect to the isopycnic mean velocity, the Stokes drift, $\overline{\mathbf{u}}^{\mathrm{S}}$, includes the bolus velocity together with the thickness-weighted gradient of $\mathbf{K}$.

REFERENCES

Andrews, D. G., and M. E. McIntyre, 1978: An exact theory of nonlinear waves on a Lagrangian mean flow. *J. Fluid Mech.,* **89,** 609–646.

——, J. R. Holton, and C. B. Leovy, 1987: *Middle Atmosphere Dynamics.* Academic Press, 489 pp.

Boss, E., and L. Thompson, 1999: Lagrangian and tracer evolution in the vicinity of an unstable jet. *J. Phys. Oceanogr.,* **29,** 288–303.

Bower, A. S., and H. T. Rossby, 1989: Evidence of cross-frontal exchange process in the Gulf Stream based on isopycnal RAFOS float data. *J. Phys. Oceanogr.,* **19,** 1177–1190.

——, ——, and J. L. Lillibridge, 1985: The Gulf Stream—Barrier or blender? *J. Phys. Oceanogr.,* **15,** 24–32.

Dukowicz, J. K., and R. J. Greatbatch, 1999: The bolus velocity in the stochastic theory of ocean turbulent tracer transport. *J. Phys. Oceanogr.,* **29,** 2442–2456.

Dunkerton, T. J., C. P. F. Hsu, and M. E. McIntyre, 1981: Some Eulerian and Lagrangian diagnostics for a model stratospheric warming. *J. Atmos. Sci.,* **38,** 819–843.

Gent, P. R., and J. C. McWilliams, 1990: Isopycnal mixing in ocean circulation models. *J. Phys. Oceanogr.,* **20,** 150–155.

——, J. Willebrand, T. J. McDougall, and J. C. McWilliams, 1995: Parameterizing eddy-induced tracer transports in ocean circulation models. *J. Phys. Oceanogr.,* **25,** 463–474.

Hayes, W. D., 1970: Conservation of action and modal wave action. *Proc. Roy. Soc. London,* **A320,** 187–208.

Haynes, P. H., and M. E. McIntyre, 1990: On the conservation and impermeability theorems for potential vorticity. *J. Atmos. Sci.,* **47,** 2021–2031.

Killworth, P. D., 1997: On the parameterisation of eddy transfer. Part I: Theory. *J. Mar. Res.,* **55,** 1171–1197.

Lee, M.-M., D. P. Marshall, and R. G. Williams, 1997: On the eddy transfer of tracers: Advective or diffusive? *J. Mar. Res.,* **55,** 483–505.

Rhines, P. B., 1977: The dynamics of unsteady currents. *Marine Chemistry,* Vol. 6, *The Sea—Ideas and Observations on Progress in the Study of the Seas,* E. D. Goldberg et al., Eds., John Wiley and Sons, 189–318.

Treguier, A. M., I. M. Held, and V. D. Larichev, 1996: On the parameterization of quasigeostrophic eddies in primitive equation ocean models. *J. Phys. Oceanogr.,* **27,** 567–580.